IN-SITU IMAGING AND SPECTROSCOPIC OBSERVATIONS OF ARTIFICIAL SHOOTING STARS. K. Kurosawa[1], H. Senshu[1], T. Kasuga[2, 1], S. Sugita[3, 1], and T. Matsui[1], [1]Planetary Exploration Research Center, Chiba Institute of Technology (kosuke.kurosawa@perc.it-chiba.ac.jp), [2]Public Relations Center, National Astronomical Observatory of Japan, [3]Dept. of Complexity Sci. and Eng., The Univ. of Tokyo.

Introduction: Two missions of the observation of shooting stars from the space, which are called Shootingstar Sensing Satelite (S^3: S-CUBE) [1, 2] and METEOR [3], have been designed by Planetary exploration Research Center of Chiba Institute of Technology (PERC/Chitech) to investigate the size distribution of meteoroids in detail.

In this study, we observed the aerodynamic interaction between particles and a surrounding gas through laboratory experiments. In-situ measurements of an artificial shooting star at point blank may provide us significant insight into the elementary steps of the energy partition during the atmospheric entry of meteoroids. Preliminary results are presented in this abstract.

Experiments: We made an artificial shooting star in a laboratory using a two-stage light gas gun at a new laboratory of PERC/Chitech [4]. A flight tube for accelerated projectiles and a chamber were filled with N_2 gas with a total pressure of 3 kPa. A polycarbonate sphere 4.8 mm in diameter was shot into the N_2 gas. Projectile velocities were 5.14 km/s (shot# 87) or 6.66 km/s (shot# 94). The velocity was measured using two laser cut sensors.

A high-speed imaging observation and a time-resolved spectroscopic observation of an artificial shooting star, observed from two directions perpendicular to the projectile trajectory, were conducted simultaneously. A high-speed video camera (Shimadzu, HPV-X) and a time-resolved spectrometer (Acton SpectraPro 300, Hamamatsu C7700) were used for these measurements. The distance between the projectile trajectory and the collecting optics of measuring instruments was ~50 cm. The fields of view (FOV) for imaging and spectroscopy were 40 mm x 62 mm and 7 mm x 18 mm, respectively. The frame rate and the exposure time for the video camera were set to 0.5 μs/frame and 0.2 μs, respectively. We used two stroboscopic lamps for shot# 87 to capture scattered light images to investigate whether the generation of melt droplets occurs within 10-20 μs. The wavelength coverage and resolution for the spectrometer were set to 360-730 nm and 5.6 nm, respectively. The sweep duration and the time resolution of the spectrometer were 19.4 μs and 0.6 μs, respectively.

Results: The results of two shots are presented in this abstract. First, we discuss the results of Shot# 94. In this shot, we captured the images and an emission spectrum of a self-luminous artificial shooting star simultaneously.

High-speed imaging: Figure 1 shows a time variation of a self-luminous projectile. Although the distance between the laser-cut sensors and the chamber is 3 m, the velocity of the projectile in the FOV of the video camera kept the initial velocity. The projectile was intact during the observation. A steady state of a gas flow was produced around the projectile at a projectile-centered frame. There is a constriction ~1 cm behind the projectile. Hereafter, we labeled the portion of the projectile, the constriction, and a wake as "Head", "Neck", and "Tail", as shown in the lowest panel of Fig. 1. The Neck was expected to be produced by a pressure gradient between the projectile trajectory and a surrounding gas.

Spectroscopy: Figure 2 shows a time-resolved emission spectrum. We detected the molecular band emission from CN Violet band system and the C_2 Swan band system. A continuum emission at >600 nm was also detected simultaneously. This continuum was expected to be emitted by small dust and or melt droplets originated from the projectile. Since the polycarbonate projectile does not contain nitrogen in its chemical structure, the CN detection is an evidence of a chemical interaction between the projectile and a surrounding N_2 gas.

Light curve: Figure 3 shows the special distributions of irradiance from the artificial shooting star. Although our spectroscopic system did not resolve the measuring object spacially, the constant

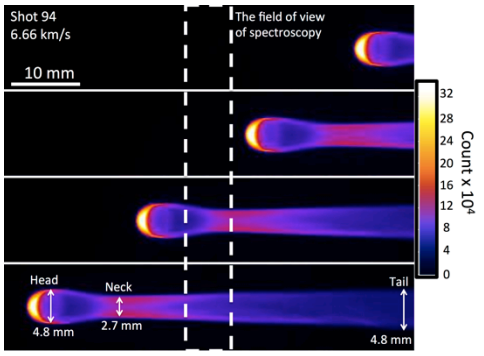

Figure 1. Examples of high-speed images. The time interval between images is 2.5 μs. The field of view of spectroscopy is shown as two dashed lines. The measured diameters of each position are also indicated in the figure.

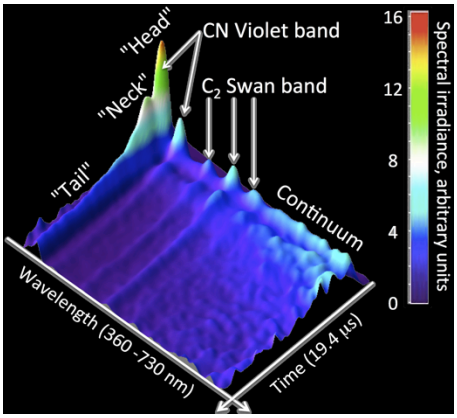

Figure 2. A time-resolved emission spectrum from Shot# 94. The detected molecular bands are shown in the figure. The spectrum was calibrated using a NIST-traceable quartz-halogen-tungsten lamp.

projectile velocity and a steady gas flow around the projectile found in the imaging observation allow to convert from the time for spectroscopic observation to the distance from the front surface of the projectile. We obtained the spatial distribution of the emission source of CN, C_2 and blackbody radiation from the spectrum. The video camera captured an irradiance integrated over the wavelength range of the visible. The comparisons clearly show that the special pattern of the irradiance observed by the video camera was produced by the molecular band emission from CN.

Blackbody temperature: We roughly measured the color temperatures at "Head", "Neck", and "Tail" with the Planck function fitting at >600 nm. Figure 4 shows the results of spectral fitting. The color temperatures at each position are close to ~3500 K. We observed no temperature decrease in this special and/or time scale.

Melt droplets: Then, we discuss the results of shot# 87. In this shot, scattered light images were obtained using the stroboscopic lamps. Figures 5abc show the time variation of the images. A melt dispersion was observed, showing that the melting of the front surface of the polycarbonate due to aerodynamic heating occurs within ~10 μs. Figure 5d shows a time-stacked image of the same shot. We roughly measured velocities and ejection angles of two melt droplets using the tracks in the figure. The dispersion velocity of the melt droplets was 45-60 % of the projectile velocity.

Discussion & Conclusions: We demonstrate in-situ observations of an artificial shooting star ~50 cm beside from the trajectory. The special distribution of the emission source around the flying projectile can be obtained. Further analysis using molecular band emission may provide the understanding the chemical interaction between the projectile and a surrounding gas.

References: [1] Ishimaru R. et al. (2013), *LPS XXXXIV*, **1944**. [2] Ishimaru R. et al. (2014), *LPS XXXXV*, **1846**. [3] Arai, T. (2014), *LPS XXXXV*, **1610**. [4] Kurosawa, K. et al., In revision.

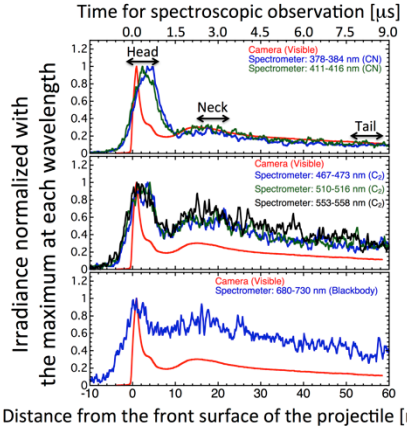

Figure 3. The spacial distribution of the emission. The integrated ranges of wavelength are shown in the figure. The position of "Head", "Neck", and "Tail" are also shown.

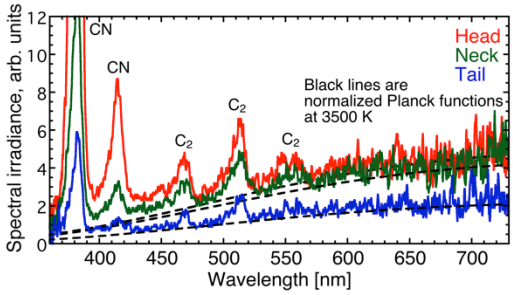

Figure 4. The results of color temperature measurements for each position.

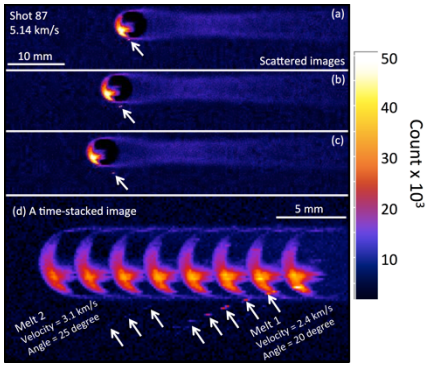

Figure 5. (a)-(c) Scattered-light images from Shot# 87. The time interval between images is 0.5 μs. Arrows in the figures indicate the position of melt droplets. (d) a time-stacked image. The track of melt droplets can be observed. The measured velocity and ejection angle for two droplets are shown in the panel (d)